Article

Journal of
Nanoscience and Nanotechnology
Vol. 17, 6307–6317, 2017
www.aspbs.com/jnn

Mineralogy and Geochemistry Characteristics and Genetic Implications for Stratabound Carlin-Type Gold Deposits in Southwest Guizhou, China

Xiaoxia Li[1,2], Xiaoqing Zhu[1,*], Yuantao Gu[1], Kunyue Ling[1], Xiangyuan Sheng[1,2], and Li He[1,2]

[1] *State Key Laboratory of Ore Deposit Geochemistry, Institute of Geochemistry, Chinese Academy of Sciences, Guiyang 550081, Guizhou, China*
[2] *University of Chinese Academy of Sciences, Beijing 100049, China*

The southwest of Guizhou Province is considered to be one of the most important areas of the Carlin-type gold deposits in China. Three deposits, Shuiyindong, Nibao and Getang which are all stratabound but with different lithology, were chosen to compare the characteristics of host strata and the source of ore-forming materials. Geochemical analyses and petrographic observation were carried out on the ores and representative minerals from the three gold deposits. Abundant pyrite in all samples can be divided into depositional pyrite and hydrothermal pyrite based on the textures and trace elements. Arsenian pyrite is the major gold-bearing minerals and mainly formed during hydrothermal processes. The involvement of the hydrothermal pyrites is closely related to the enrichment of gold, in which the fluid should be enriched in Au and As, but depleted in Fe. Specially, the gold element presented in these Carlin-type gold deposits often occurred in invisible forms including nanoparticles, submicroscopic particles and crystal lattice. Nanoparticles and submicroscopic particles of Au mostly emerged in the arsenian pyrite and quartz voids, which suggested that pyritization and silicification take place during the main mineralization stage. High contents of lattice Au mainly exist in the overgrowth rims of arsenian pyrite. In addition, mineralized rocks of the Shuiyindong, Nibao and Getang deposits display LREE enrichment patterns. And the samples from Shuiyindong and Nibao deposits exhibit similar geochemical behavior as those from the samples of typical Emeishan basalt, indicating that these two deposits may be affected by basic volcanic clastic material during sedimentation. However, the ore-forming materials of the two deposits are different. The Shuiyindong deposit likely result from the mixtures of magmatic source with minor contribution of sedimentary rocks, whereas the Nibao deposit might have a magmatic source. The element geochemistry of samples from Getang deposit is much different from the other two deposits, and the sedimentary rocks may be the major contribution. As a consequence, the synthesized studies on these three deposits significantly contribute to a better understanding of the ore-forming materials source and the formation process of these nano- and submicron gold particles of Carlin-type gold deposits in the southwest Guizhou Province, China.

Keywords: Stratabound, Carlin-Type Gold Deposit, Arsenian Pyrite, Invisible Gold, Ore-Forming Materials, Nano-Au.

1. INTRODUCTION

Carlin-type gold deposits were initially found in Nevada, in the United States.[1–3] Compared with other kinds of gold deposits, it has unique features such as that: orebody is disseminated and hosted by carbonate rocks; Au is always present as submicronsized particles or solid solution, which is inside or close to disseminated pyrite and arsenopyrite.[4] The presence of disseminated Au deposit in the southwest (SW) of China has been recognized since the 1970s, and the Banqi gold deposit is the first Carlin-type gold deposit discovered in China.[5,6] Since then, more than 200 Au mineralized deposits with mineral reserves/resources ranging from 1 to 167 tons in this type have been defined in this district. The grade of

*Author to whom correspondence should be addressed.

these deposits is different from each other, mostly ranging from 1 to 20 g/t.

The southwest of Guizhou Province is one of the most important producers of Carlin-type gold deposits in China, such as Shuiyindong, Lannigou, Zimudang and Nibao. These deposits are generally divided into two kinds. One is structurally controlled gold deposits (e.g., Lannigou, Yata, Banqi) which always present at high angle fracture zones and the stratigraphic units are commonly Middle to Lower Triassic argillaceous. The other one is stratabound gold deposits (e.g., Shuiyindong, Taipingdong, Nibao). These deposits are mainly hosted by the Upper Permian strata and the depositional discontinuity surface between the Middle and Upper Permian.[7]

Many previous studies on Carlin-type gold deposits attempted to illuminate the deposit genesis and the migration and precipitation of the gold. To date, two genetic models were proposed:

(1) the magmatic source: ore-forming fluids and metallogenic materials come from magmatic hydrothermal fluid or deep metamorphic fluid, followed by unloading and precipitating far from the magmatic rock, which means that gold may derive from mantle or deep crust, and the lithology, tectonic conditions of ore-bearing stratum are advantageous to trapping the elements;[8–10]

(2) the amagmatic source: gold may derive from the ore-bearing stratum or hydrothermal solution, in which the ore-forming elements can migrate and precipitate by water-rock reactions, or be leached by meteoric water from Paleozoic strata, and then precipitate and enrich in the shallow earth crust.[5, 11–14]

All of the ore-forming elements (such as Au, As, Sb, Hg etc.) are in anomalous abundance in this region. If the anomaly represents the real enrichment and happens prior to the Carlin-type gold deposit mineralization, it is possible that much or all of the gold would be derived relatively locally from the host rocks. Otherwise, the gold may derive from deeper in the circulation path. Especially for the stratabound Carlin-type gold deposits, the stratabound characteristic make host rocks more likely to contribute to its ore-forming materials. Several works have already been done to suggest that specific wall rocks may be considered as a source for the Au and other metal materials in the deposits.[15–17] In contrast to those above mentioned, the migration and precipitation of the gold of the Carlin-type gold deposits were relative lag behind. Also, previous studies have pointed out that, with Carlin-type gold deposits in Nevada, the mainly mode of occurrence of gold is solid solution (Au^{1+}) and/or native gold particles (Au^{0+}) within nano to micron scales.[11, 18–21] As to the specific characteristic of the Carlin-type gold deposits in southwest of Guizhou Province, the uncertainties are still remaining. Specially, the study of the precipitation mechanism of these abundant and unique nano-submicron gold particles has not received enough attention.

To certify the genetic implications and the formation process of these nano and submicron gold particles of Carlin-type gold deposits in southwestern Guizhou Province, we investigated the Shuiyindong, Getang and Nibao gold deposits and discussed the differences of the three gold deposits from the following three aspects:

(1) the texture and genesis of arsenian pyrite,
(2) occurrence and distribution of invisible gold,
(3) elements geochemistry.

2. REGIONAL GEOLOGY AND DEPOSIT GEOLOGY

2.1. Regional Geology

The southwestern Guizhou Province, which is at the boundary of Yunnan Province and the Guangxi Autonomous Region, is one of the most important parts of the Dian-Qian-Gui "Golden Triangle" and locates on the juncture of the Yangtze Block and the Youjiang fold belt. In this area, the tectonics developed very well and was controlled by several first-order structures, like Mile-Shizong, Gejiu-Binyang and Ziyun-Yadu faults.[22]

In this region, the gold deposits distribute either in the isolated carbonate platforms or near the southwest margin of Youjiang basin. The ore-bearing strata range from Devonian to Triassic, and the Triassic rocks are commonly distributed. Exposed and drilled strata in this area mainly consist of the Middle Permian Maokou Formation (P_2m) composed of limestone; the Dachang Formation (P_2dc), a set of siliceous rocks like silicified breccia and silicified argillite (also called STB); the Emeishan basalt Formation ($P_3\beta$) which consists of tuff and sedimentary tuff; the Upper Permian Longtan (P_3l) and Changxing Formation (P_3c) composed of calcareous siltstone, bioclastic limestone, siltstone and intercalated with coal seams occasionally, and unconformably overlain the Maokou Formation. The Triassic strata mainly consist of the Lower Triassic Yelang (T_1y) and Yongningzhen Formations (T_1yn). The Yelang Formation consists of argillite, argillaceous limestone, marlstone and siltstone etc. The Yongningzhen Formation is dolomite and limestone interbedded with argillaceous limestone. All of them are the main gold-bearing strata except the Maokou Formation and the Yongningzhen Formation. The orebodies are hosted mainly by Late Permian to Triassic limestone and various impurity carbonate rock and clastic rock. Magmatic rocks is not widely distributed in the area, only present along with the Devonian to Early Triassic strata in few places and some small-scale ultrabasic, basic and intermediate-acid rocks that intruded Late Yanshanian Orogeny.[5, 23]

After the Caledonian tectonic movement, a set of sediments deposited thickly and broadly in Youjiang Basin from the Devonian to the Triassic and are subdivided into two stratigraphic sequences according to the difference of their sedimentary facies, which belong to the

Youjiang Basin and the Yangtze passive continental margin, respectively.[14]

The stratigraphic sequence located on the Youjiang Basin is mainly distributed in Middle Triassic and characterized with a set of deep marine facies terrigenous clastic turbidite. The terrigenous clastic rocks are the predominant formation for gold, also called the Laizishan Sequence, named by Han et al.[24] and Wang.[25] Representative gold deposits include Lannigou, Yata and Jinya gold deposits etc. Another stratigraphic sequence that belongs to the Yangtze Block is unconformity overlain between the Maokou Formation (P_2m) and the Laishike Formation (T_3ls). Wang[25] also first named this gold-bearing sequence as the Longtoushan Sequence.[25] And it is the most important stratigraphic for gold in the southwestern Guizhou Province. It is a set of marine carbonate rocks, interbedded lots of terrigenous clastic rocks and volcanic rocks, which are important gold-bearing unit. Terrigenous clastic rocks mainly distributed in the Longtan and Yelang Formation and the representative gold deposit is the Shuiyindong gold deposit. Volcanic rocks that distributed in the Dachang and Emeishan basalt Formation are the main host rocks for the Getang and Nibao gold deposits.

2.2. Deposit Geology

The deposits in this study are the same subclass of Carlin-type deposits that were defined above, which are all distributed in the Yangtze Block and belong to the Longtoushan Sequence (Shuiyindong, Nibao, Getang). Moreover, they have some similarities in the ore body, ore-bearing strata and the structures that control the whole deposit.[7] The Shuiyindong and Nibao deposit are stratabound and structurally controlled complex deposit, while Getang deposit is typical stratabound. All of their ore bodies have an obvious anticlinal ore-controlling feature. The ore-bearing strata are from Permian to Triassic, and have a close relationship with the unconformity. The basements of the unconformity are all the Middle Permian Maokou Formation (P_2m). The host rocks are in different lithology as mentioned above. The Shuiyindong deposit is mainly hosted in the impure carbonate rocks of the Permian Longtan Formation; the Nibao deposit is closest to the Emeishan basalt, and the main ore-bearing formation is the Emeishan basalt formation ($P_3\beta$), which is on the top of the Maokou Formation (P_2m) and composed of tuff, tuffaceous siltstone and so on; the Getang deposit is major in Dachang Formation (P_2dc), and the main host rocks are argillite and siliceous limestone.[26] The locations of the three deposits are shown in Figure 1.

2.2.1. The Shuiyindong Deposit

The Shuiyindong Au deposit is located approximately 20 km northwest of the town of Zhenfeng Country, in southwestern Guizhou Province. The deposit lies on the eastern part of the Huijiabao anticline which is located

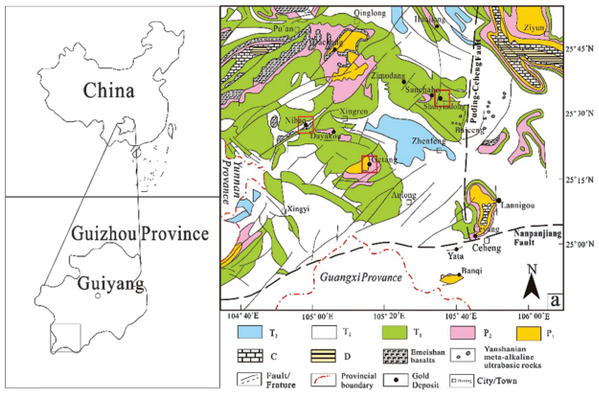

Figure 1. Simplified regional location of the SW of Guizhou Province (modified after Zhang et al.[27]).

at the southwest margin of the Yangzi paraplatform, controlled by the structure and favorite lithology of the Huijiabao anticline.[28, 29] The orebodies mainly are stratiform hosted by the Permian Longtan Formation (Fig. 2). The wall rocks of the deposit are mainly bioclastic limestones interbedded with tuffaceous material. As the main ore rock, impure carbonate rocks have much higher Au content. Because of the alternate change of permeability differences, argillite, bioclastic limestone, calcareous siltstone and silty argillite form a set of lithological association that is in favor of mineralization. In addition, silicification, decarbonatization and pyritization have a close relationship with gold mineralization.

2.2.2. The Nibao Deposit

The Nibao Au deposit is in the south of Pu'an Country, Guizhou Province, located at the north boundary of the Yangtze Block and Youjiang orogenic zone, and mainly occur in tuff area which is the outer edges of the Emeishan basalt area. Nibao anticline and Erlongqiaobao anticline are the main structures that control the output and distribution of the Nibao gold deposit.[30] According to the spatial

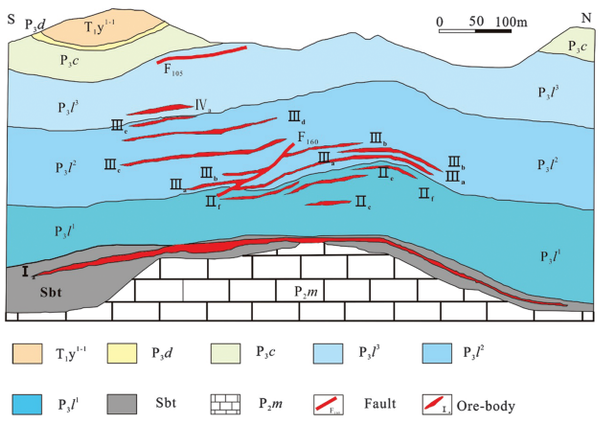

Figure 2. Cross section maps of Shuiyindong gold deposit (modified after Liu et al. (2005)[28]).

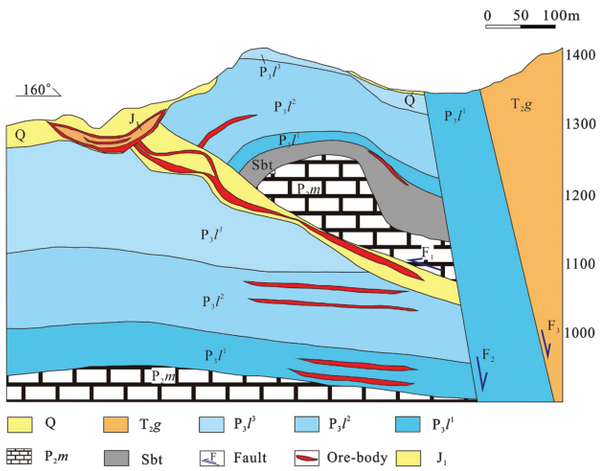

Figure 3. Cross section maps of Nibao gold deposit (modified after Zheng et al.[31]).

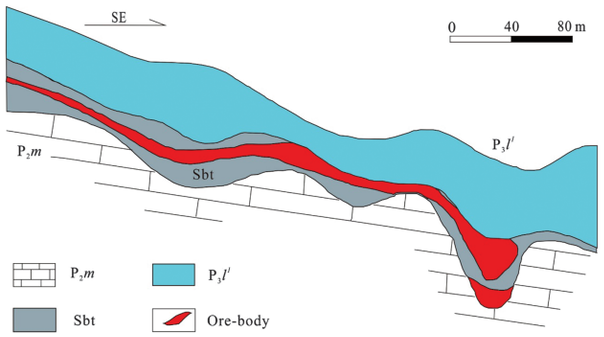

Figure 4. Cross section maps of Getang gold deposit (modified after Huang et al.[33]).

location and the ore-controlling factors, the ore-bodies are divided into stratabound and structurally controlled. Sedimentary rocks in the mining area are dominated by the Middle Permian Maokou Formation (P_2m), the Upper Permian Longtan Formation (P_3l) and Emeishan basalt formation ($P_3\beta$) (Fig. 3). The Emeishan basalt formation is the most important gold-bearing strata, distributed in northwest part of Erlongqiaobao antiline and the eastern part of the mining area, which are mainly comprised of sedimentary tuff. The Upper Permian Longtan Formation is the secondary gold-bearing strata. Alteration that related to the gold mineralization at the Nibao gold deposit is silicification and sulfidation.[31]

2.2.3. The Getang Deposit

The Getang Au deposit is in An'long Country, Guizhou Province and also located at the southwest margin of the Yangzi paraplatform. The deposit lies on the southeast of the Getang antiline, controlled mainly by the dome and box antiline. The ore-bodies are almost 10°-dipping and near-horizontal layers and controlled mainly by the decollement structure. The ore-bodies are mostly distributed on the unconformable surface between the Maokou Formation and the Upper Longtan Formation (Fig. 4), which consists of a set of structure alteration rocks called Dachang Formation. Some researchers also named this set of rocks as SBT, and demonstrated that it is formed through hydrothermal alteration and generally characterized by silicification consisting of silicified breccia and silicified argillite.[32] The main host strata in the Getang deposit are the Upper Permian Longtan Formation and the Lower Permian Maokou Formation, surrounded by Changxing, Dalong Formation and Triassic Yelang Formation.[33] The Upper Permian Longtan Formation (P_2l) is comprised of a set of terrigenous clastic rocks, which are the main host rocks of gold. Silicification, pyritization and ferritization are very common in the Getang Au deposit. Silicification and pyritization are the products of tectonism and hydrothermal alteration, commonly found in primary ores, while ferritization mainly occurs in shallow oxidized ores, formed by the supergene alteration.

3. SAMPLING AND ANALYTICAL METHODS

For this study, the samples were collected from either tunnels or stopes. According to the main deposit host rock types of the three deposits, most of our samples are collected in different lithology. Samples collected from the Shuiyindog, Getang, and Nibao gold deposits are mainly bioclastic limestones, silicified rocks, and tuff and alloclastic breccias, respectively. Furthermore, we collect some typical Emeishan basalt from Luodian, Fule and Tianba. The lithology of the samples is listed in Table II. Most of the measurements were performed at the State Key Laboratory of Ore Deposit Geochemistry, Institute of Geochemistry, Chinese Academy of Sciences (Guiyang). Gold and mercury were analyzed by ALS-Chemex (Guangzhou) commercial laboratories.

All the whole-rock samples were crushed and then ground to 200 meshes for ICP-MS analysis for the Au, As, Hg, and other trace-elements composition. The trace and REE elements were analyzed by Perkin-Elmer Sciex ELAN 6000 ICP-MS. Typically, 50 mg powdered samples were weighed and dissolved by acid, and measured by internal standard method. The analytical precision was generally better than 5% for all elements, and more detailed methods were described by Qi and Gregeire.[34]

Thin sections were made for all the samples and observed under the polarizing microscope. Some representative samples were chosen for backscattered electron (BSE) imaging and EMPA of arsenian pyrite. JSM-7800F (JEOL, Japan) field emission scanning electron microscope was used to observe the mineral morphology and an energy dispersive spectrometer (EDS) on the FE-SEM was used to identify minerals.

Chemical analyses of pyrite and arsenian pyrite were performed on EPMA-1600 (Shimadzu, Japan) electron probe microanalyzer. Fe, S, As, Au, Sb, Ag, Cu, Zn, Co,

Se, Te and Ni were detected using a 25 keV accelerating voltage, 25 nA beam current, and a 10 s-counting time. The detection limit of all elements is 300 ppm, with exception of 500 ppm for S and 400 ppm for Au in arsenian pyrite. The analytical precision was also better than 5%.

4. RESULTS AND DISCUSSION

4.1. Pyrite Texture and Trace Element Chemistry

According to the observation by the optical microscopy and BSE, we can divide the pyrite into two types of genesis: depositional pyrite and hydrothermal pyrite. Hydrothermal pyrite grains, as the major host for gold in Carlin-type gold deposits, in all of the three deposits have clear zonal textures. In general, depositional pyrite is always formed as a core pyrite with disseminated or isolated grains in the ores.

Depositional pyrite in the Shuiyindong gold deposit varies in textures and can be divided into two types. Framboidal pyrite grains, which is generally thought to be nucleated rapidly of the mineral at low temperatures, are mostly synsedimentary or earlier than diagenetic in origin (Fig. 5(B)).[35] Subhedral-euhedral pyrite grains distributed in the host rocks are the most common grains in all samples, and they are commonly 10–100 μm in size with low gold contents. Hydrothermal pyrite occurs as bioclastic pyrite grains and tiny fine-grained pyrite or colloidal pyrite (Figs. 5(A, C)). Bioclastic pyrite grains are formed by tiny subhedral to anhedral pyrite, which is formed during later hydrothermal event that replace or fill early biodetritus and retain their morphology (Fig. 5(I)). The colloidal pyrite always has different thickness overgrowth rims with high content of As (3.58 wt.%–9.45 wt.%) and Au (1100–3900 ppm). In the Nibao and Getang gold deposits, the depositional pyrite mainly present as grains and tiny fine grains or framboidal pyrite (Figs. 5(D, G, H)), respectively. Most of the hydrothermal pyrites in Nibao gold deposit are distributed in the cement in tuff clastic and are subhedral-euhedral zoned grains (Fig. 5(E)). In the Getang gold deposit, hydrothermal pyrite occurs as cubic crystal and little of them have overgrowth rims (Fig. 5(I)).

Arsenian pyrite is the main gold-bearing mineral in all of the three deposits, especially the Shuiyindong gold deposit. The main characteristics of element distribution are that overgrowth rims always have a higher content of As and Au than those of core pyrite. Meanwhile, detailed analyses point out that a positive correlation exists between Fe and S (Fig. 6). EPMA analyses show that, the average value of S/Fe of arsenian pyrite from all of the Shuiyindong and Nibao deposits is 1.91, indicating that As may substitute for S as As^{1-} into the pyrite and form $Fe(As, S)_2$.[36, 37] A negative correlation between As and S (Fig. 7(a)) is also in agreement of this result. In addition, a weak negative relation has also been revealed between As and Fe from analysed samples, which may indicate the substitution of As for Fe (Fig. 7(b)). Moreover, certain As-rich pyrite have more than one overgrowth rims with different width, which indicates that the ore forming fluids have a compositional variation during the evolutionary process. Furthermore, previous studies about other Carlin-type gold deposits in southwest of Guizhou also suggested that the enrichment of gold was

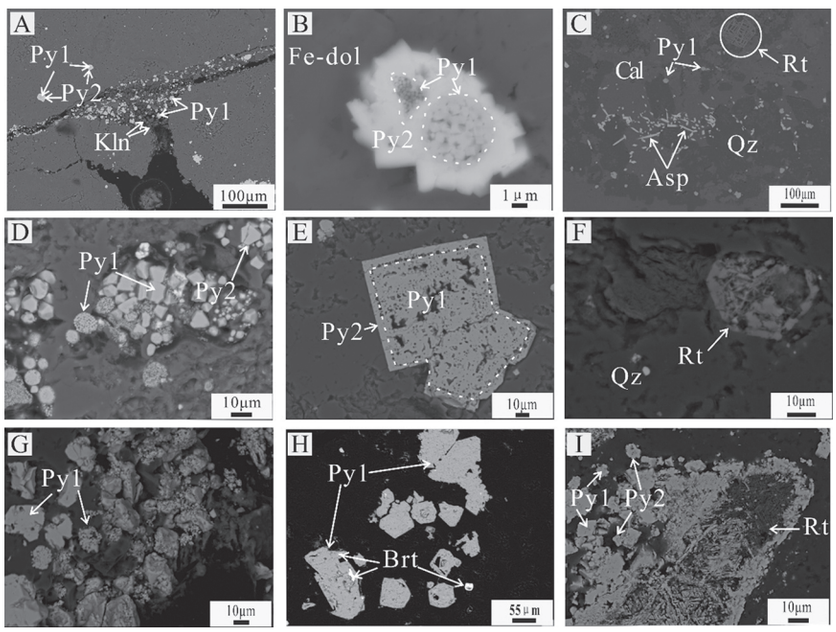

Figure 5. Backscattered electron (BSE) images showing arsenian pyrite textures from the Shuiyindong (A–C), Nibao (D–F) and Getang gold deposit (G–I) Qz-quartz; Cal-calcite; Fe-dol-ferroan dolomite; Kln-kaolinite; Rt-rutile; Brt-barite; Asp-arsenopyrite; Py1-depositional pyrite; Py2-hydrothermal pyrite.

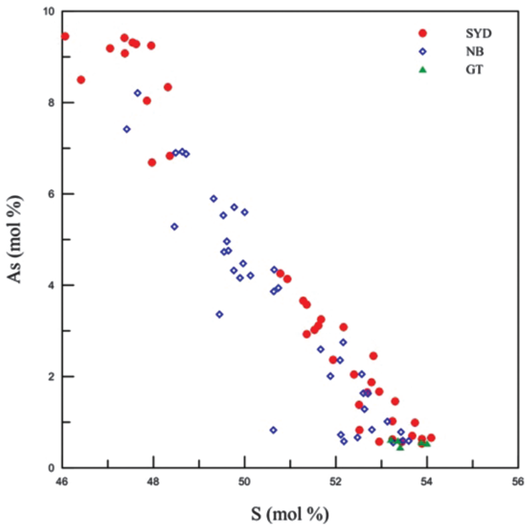

Figure 6. Elemental relationship of As versus S for EMPA analyses from the Shuiyindong, Nibao and Getang gold deposits.

closely related to the pyrites involved in the hydrothermal influence. For instance, in another super large Lannigou Carlin-type gold deposit, the distribution of trace element indicates that the periodicity enriched-depleted element zoning of the As-rich pyrite may be ascribed to the changed solubility of gold resulting from the periodicity pressure dropping of the hydrothermal fluid. In particular, the Au content can reach up to 990 ppm, coupled with As, Sb, Tl, Cu and Bi in pyrite overgrown rims, a combination with basin fluid character.[38] Hou et al.[39] also proposed that the gold is mainly distributed in the Py3 and Py4 with concentrations up to 110 ppm and 810 ppm, and the gold was introduced during the hydrothermal fluid in the Huijiabao trend in Guizhou Province based on the trace element of the multiple-stages pyrites.[39] Based on the electron microprobe analyses, arsenian pyrite and pyrite grains from the three deposits contain minor elements of As, Au, Se, Ni, Co, Sb, Te, Zn, Ag and Cu. Among these minor elements, arsenic is the most abundant, usually 0.5 wt.%–9.451 wt.% (Table I). The arsenian pyrite from Shuiyindong gold deposit has the highest content of As, (4.06 wt.%), followed by Nibao deposit (3.30 wt.%) and Getang deposit (0.55 wt.%). The concentration of Au, Ni and Cu are near the detection limits. The three elements in the Shuiyindong and Nibao are little more abundant than Getang deposit, and the concentration of other elements are below the detection limits. The content of Co in the samples from three deposits are either below the detection limit or not measured, except for specific pyrite from Nibao deposit in which the Co/Ni value is greater than 1.5, meaning that the ore-forming process may be affected by magmatic hydrothermal. Previous researches have mentioned that the value of Co/Ni in the pyrite from Getang gold deposit is also greater than 1, which suggests hydrothermal reconstructed after sedimentation.[33, 40]

4.2. Distributions of Gold in Arsenian Pyrite

Previous studies on the gold occurrence of Carlin-type gold deposits in the southwest of Guizhou proposed that the gold is mainly hosted in pyrite and arsenopyrite with main existing forms of micro-submicroscopic particles and nanoparticles.[7, 41] In this study, three types of gold were observed in the Carlin-gold deposits of the southwestern Guizhou Province:

1. Au presents in the growth bands of arsenian pyrites as crystal lattices, which may result from the water-rock reaction;
2. Au occurs as nanoparticles in arsenian pyrite veinlet or quartz;
3. Au is hosted in the veinlet or the fractures of pyrites as submicroscopic particles.

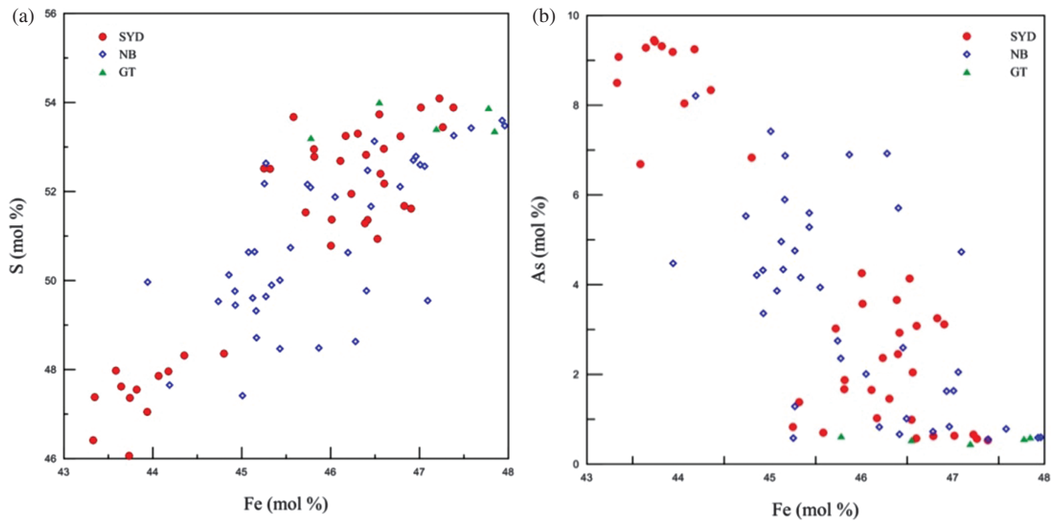

Figure 7. Elemental relationship of (a) Fe versus S and (b) Fe versus As for EMPA analyses from the Shuiyindong, Nibao and Getang gold deposits.

Table I. The summary of the EMPA analyses of pyrite from Shuiyindong, Nibao and Getang deposits (in wt.%) bdl-below detection limit.

Sample	S	Fe	As	Au	Se	Ni	Co	Sb	Te	Zn	Ag	Cu	
Detection limit	0.05	0.03	0.03	0.04	0.03	0.03	0.03	0.03	0.03	0.03	0.03	0.03	Total
Shuiyindong $N = 39$													
Min.	46.06	43.33	0.53	0.04	bdl	bdl	bdl	bdl	bdl	bdl	bdl	bdl	98.77
Max.	54.09	47.38	9.45	0.39	0.07	0.21	bdl	0.07	0.07	0.04	0.04	0.10	102.10
Mean	50.99	45.59	4.06	0.19	bdl	0.05	bdl	bdl	bdl	bdl	0.01	0.05	100.82
Nibao $N = 39$													
Min.	47.41	43.94	0.51	bdl	bdl	0.00	bdl	bdl	bdl	bdl	bdl	bdl	97.82
Max.	53.60	47.96	8.21	0.13	0.06	0.30	0.11	0.05	0.07	0.25	0.04	0.63	102.30
Mean	50.74	45.92	3.30	0.06	bdl	0.03	bdl	bdl	bdl	bdl	bdl	0.08	100.05
Getang $N = 5$													
Min.	53.21	45.78	0.45	bdl	bdl	bdl	bdl	bdl	bdl	bdl	bdl	bdl	99.70
Max.	54.00	47.85	0.62	0.07	bdl	0.03	bdl	bdl	0.04	bdl	bdl	bdl	102.31
Mean	53.57	47.03	0.55	0.07	bdl	bdl	bdl	bdl	bdl	bdl	bdl	bdl	100.96

In the samples from Shuiyindong gold deposit, several native gold grains were observed in arsenian pyrite veinlet and denoted by circles in Figures 8(B), (C). The size of the native gold is about 1 μm. The native gold particles distributed either in the edges of arsenian pyrite or scattered in the arsenian pyrite grains. The distribution of native gold may imply the gold precipitation mechanism. The gold particles that distributed near or in the arsenian pyrite overgrowth rims were formed later than the arsenian pyrite and may be exsolved from metastable arsenian pyrite caused by a later hydrothermal event.[20] The other situation is Au particles scattered among the arsenian pyrite grains, which may by formed at the same time with arsenian pyrite as a consequence of exceeded solubility limit of gold in the hydrothermal fluid.[20,41] In addition, we also found native gold in the sample from the Getang gold deposit (Figs. 8(D, E)). It consists of three nanoparticles (about 30 nm) which were distributed in the edge of quartz particles and near the voids that may be created by mineral dissolution. These results suggest that the gold mineralization is related to not only the pyritization but also the main stage of silicification.

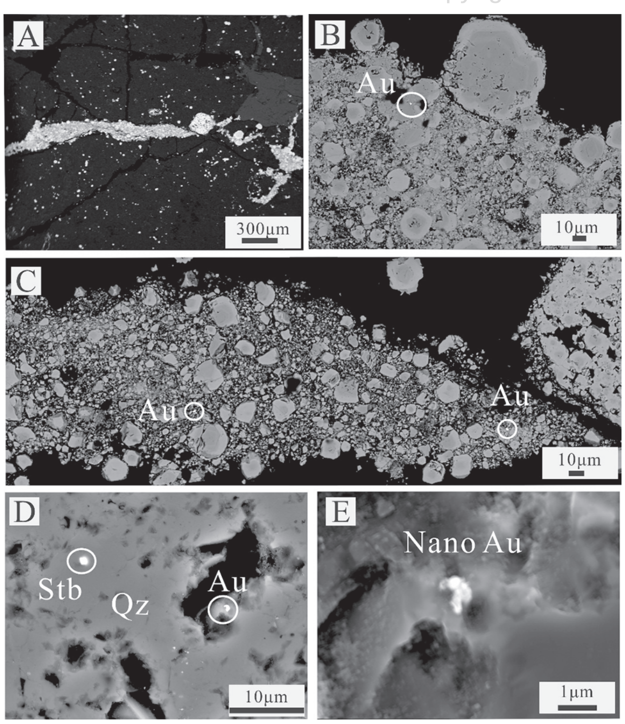

Figure 8. Backscattered electron (BSE) images showing the distribution of native gold (A–C) Arsenian pyrite veinlet from the Shuiyindong gold deposit; (D, E) quartz particles from the Getang gold deposit Qz-quartz; Stb-stibnite.

Furthermore, the EMPA and EDS analyses show that Au have been detected in arsenian pyrite from all of the three deposits, and mainly in the forms of invisible gold with contents of Au as high as 400–3900 ppm. It is noteworthy that high contents of As, ranging from 3.58 to 9.45 wt.%, exist in the overgrowth rims, in which Au has the most abundance with content ranging from 1100–3900 ppm. In this case, it is considered that gold may occur not only as micron to submicron particles but also in lattice of pyrite. According to previous studies, it is well known that Au mostly migrate in Au^{1+} or Au^0 forms in Carlin-type gold deposits.[19–21] There is a upper solubility limit for Au in pyrite that has been established by Reich et al.:[21] for a range of temperature between 150 and 250 °C, $C_{Au} = 0.02 \times C_{As} + 4 \times 10^{-5}$ (mol%).[21] When the Au/As ratios are above 0.02, it reached saturation in solutions and Au presents as Au^0 nanoparticles.[19,21] Otherwise, the dominant form is Au^+, occurring as solid solution in pyrite. These two existent forms of Au may be serious affected by the saturability of gold-bearing fluid.[19,21] Moreover, Su et al.,[28] analyzed the fluid inclusions from the Shuiyindong deposit for the major ore forming stage and showed that the dominant Au species were $Au(HS)^{2-}$ (77 %) and $AuHS^0_{(aq)}$ (23 %), and found no gold-hydroxyl and gold-chloride complexes.[28] Previous studies have confirmed that Au^{1+} was much stable than Au^{3+}, and Au^{3+} was easily reduced to Au^{1+} or Au^0.[42] Dissolved Au could combine with S or As and then form complexes chemisorbed at As-rich, Fe-deficient sites in the arsenian pyrite.[43,44] Negatively charged $Au(HS)^{2-}$ complexes can be adsorbed on semi-conducting As-pyrite or arsenopyrite surfaces electrochemically, or Au^{3+} and Au^{1+}

Table II. Rare earth element and trace element compositions in Shuiyindong, Nibao and Getang gold deposits ($\times 10^{-6}$).

Lithology	Tuff		Basalt						Impure carbonate rocks								Siliceous rock			
Sample	NB-01	NB-04	NB-06-01	NB-06-02	NB-09	Yin-1-10	FLC	TB	SYD-03	SYD-04	SYD-07	SYD-08	SYD-09	SYD-12	SYD-13	SYD-14	GT-01	GT-02	GT-05	GT-08
Sc	21.10	6.22	25.20	23.80	27.20	30.26	29.83	26.82	19.34	16.25	12.38	15.30	21.23	8.68	11.78	9.63	2.26	2.68	1.93	1.99
Cr	77.20	378.76	62.60	74.90	333.64	45.00	70.20	40.20	209.00	77.50	113.00	141.00	85.00	57.70	127.00	78.80	29.40	26.40	20.40	35.10
Ni	39.30	403.00	58.20	70.90	92.50	57.10	66.71	45.16	79.68	69.89	31.60	46.11	40.87	30.22	38.12	44.65	6.94	16.66	3.80	36.06
Ga	24.70	21.80	19.50	25.80	23.40	23.40	23.70	22.40	24.30	24.00	18.10	17.70	29.00	7.93	8.83	7.73	1.47	1.33	0.99	1.26
Rb	106.00	60.02	5.16	7.02	13.97	0.99	4.89	30.00	78.80	78.90	38.80	54.10	88.70	21.70	27.90	33.20	1.57	1.87	0.67	2.63
Sr	44.10	335.00	620.00	380.00	515.00	194.00	323.00	334.00	244.00	361.00	293.00	478.00	355.00	582.00	588.00	561.00	99.00	91.60	78.90	34.40
Ba	115.00	128.00	406.00	184.00	132.00	56.30	308.00	297.00	572.00	641.00	289.00	346.00	620.00	188.00	240.00	205.00	30.30	24.30	16.00	10.50
Y	29.90	32.20	32.00	34.60	33.00	35.90	34.90	36.50	26.40	35.10	26.80	24.10	41.50	22.00	36.00	27.20	3.03	4.42	1.15	2.30
Zr	313.00	456.06	224.00	280.00	322.41	350.70	263.59	371.06	345.04	425.37	192.32	222.86	481.93	156.12	174.22	187.79	29.19	23.98	9.85	16.52
Nb	44.66	50.51	33.00	40.82	36.23	36.83	29.66	32.90	43.14	47.76	25.04	30.66	59.01	19.80	18.64	23.19	0.41	0.38	0.27	0.50
Hf	6.62	9.12	4.39	5.76	7.17	9.64	7.19	11.28	9.82	13.04	5.57	5.78	14.70	4.67	4.89	5.53	0.72	0.60	0.36	0.36
Ta	6.90	3.54	4.88	6.45	2.34	2.25	1.84	2.22	2.64	3.46	1.44	1.83	3.99	1.38	1.12	1.43	0.04	0.07	0.05	0.11
Pb	6.13	22.90	3.18	3.87	7.33	4.97	3.56	5.78	11.20	4.24	5.25	5.07	8.01	3.56	1.36	4.64	0.20	1.63	0.26	5.90
Th	5.05	12.20	3.98	5.27	5.88	5.57	4.17	6.49	7.40	12.40	4.25	4.20	11.30	3.29	2.60	4.16	0.55	0.42	0.30	0.35
U	1.50	6.41	1.28	1.51	1.12	1.25	0.90	1.51	1.98	3.25	2.22	0.88	2.75	3.36	2.26	4.48	2.68	2.90	1.60	4.69
La	47.60	60.60	38.90	45.50	43.80	40.80	34.00	40.10	51.40	75.30	43.40	40.30	88.40	40.10	53.30	48.20	6.28	5.25	3.42	3.27
Ce	90.30	113.00	81.50	95.00	112.00	97.90	78.80	90.60	107.00	151.00	84.80	81.80	175.00	82.50	103.00	101.00	9.68	7.32	5.82	5.00
Pr	11.10	12.80	10.30	12.30	11.50	12.90	10.60	12.20	13.90	19.90	11.20	10.50	22.00	10.90	15.50	13.30	1.13	0.90	0.73	0.64
Nd	40.60	46.30	43.20	49.60	46.90	52.50	44.90	51.00	55.30	77.00	44.60	40.90	82.80	43.50	63.90	52.40	3.74	2.94	2.44	2.14
Sm	5.45	6.66	8.38	9.36	9.42	11.00	9.88	11.20	10.50	14.10	8.30	7.93	15.00	7.50	12.30	9.81	0.49	0.49	0.39	0.33
Eu	1.36	1.15	2.59	2.95	2.74	3.13	3.16	3.27	2.20	2.91	1.88	2.47	3.30	1.61	2.46	1.89	0.13	0.14	0.07	0.07
Gd	3.23	4.61	7.30	7.71	8.16	9.11	8.70	9.72	7.47	9.15	5.24	5.83	10.42	5.27	8.46	6.63	0.37	0.45	0.28	0.27
Tb	0.55	0.86	1.20	1.32	1.30	1.40	1.28	1.47	1.25	1.57	0.95	0.92	1.83	0.93	1.49	1.16	0.07	0.08	0.03	0.04
Dy	3.92	5.09	6.09	6.57	6.59	8.35	7.75	8.80	6.92	9.10	5.60	5.44	10.60	5.41	8.52	6.73	0.42	0.40	0.20	0.27
Ho	0.98	1.19	1.13	1.28	1.32	1.53	1.50	1.71	1.33	1.76	1.16	1.07	2.04	1.01	1.65	1.35	0.08	0.10	0.03	0.05
Er	3.35	3.64	3.10	3.59	3.52	3.98	3.86	4.22	3.64	4.86	3.19	2.72	5.75	2.59	4.40	3.39	0.25	0.28	0.10	0.20
Tm	0.51	0.53	0.39	0.51	0.47	0.52	0.53	0.58	0.47	0.65	0.43	0.36	0.75	0.36	0.58	0.42	0.03	0.04	0.01	0.03
Yb	3.29	3.40	2.42	2.92	2.78	3.15	3.09	3.53	2.81	3.68	2.36	2.11	4.52	2.15	3.24	2.65	0.21	0.18	0.07	0.17
Lu	0.48	0.52	0.35	0.42	0.40	0.45	0.41	0.50	0.38	0.52	0.36	0.28	0.67	0.30	0.49	0.36	0.03	0.03	0.01	0.02
ΣREE	242.62	292.54	238.86	273.63	283.89	282.62	243.36	275.39	290.96	406.59	240.26	226.73	464.58	226.12	315.30	276.49	25.94	23.01	14.77	14.79
LREE	196.41	240.51	184.87	214.71	226.36	218.23	181.34	208.37	240.30	340.21	194.18	183.90	386.50	186.11	250.46	226.60	21.46	17.03	12.87	11.45
HREE	46.21	52.03	53.98	58.92	57.53	64.39	62.02	67.02	50.66	66.38	46.08	42.83	78.07	40.01	64.84	49.89	4.48	5.97	1.90	3.34
LREE/HREE	4.25	4.62	3.42	3.64	3.93	3.39	2.92	3.11	4.74	5.12	4.21	4.29	4.95	4.65	3.86	4.54	4.79	2.85	6.77	3.43
LaN/YbN	10.38	12.78	11.53	11.18	11.30	9.29	7.89	8.15	13.12	14.68	13.19	13.70	14.03	13.38	11.80	13.05	21.76	21.04	34.85	13.72
δEu	0.91	0.60	0.99	1.03	0.93	0.93	1.02	0.93	0.72	0.73	0.81	1.06	0.77	0.74	0.70	0.68	0.92	0.90	0.59	0.69
δCe	0.93	0.95	0.98	0.97	1.20	1.04	1.01	0.99	0.96	0.94	0.92	0.95	0.95	0.95	0.87	0.96	0.82	0.76	0.86	0.80

Notes: $\delta\ \mathrm{Eu} = \mathrm{Eu}_N/[1/2(\mathrm{Sm}_N + \mathrm{Gd}_N)]$; $\delta\mathrm{Ce} = \mathrm{Ce}_N/[1/2(\mathrm{La}_N + \mathrm{Pr}_N)]$.

precipitate due to Au reduction.[45, 46] Although there are differences in the ore-forming materials among the three deposits, they exhibit a lot of same characteristics, like chemistry of gold-bearing minerals and alteration types. In the southwestern Guizhou Province, decarbonatization and sulfidation are the most important alteration types and closely related to the mechanisms of gold precipitation. According to the studies of fluid inclusions and mass transfer during mineralization and alteration from Shuiyindong deposit, the ore-forming fluids were poor with Fe but possibly rich in sulfur, while the sedimentary rocks contain more Fe than that needed to combine with all of the sulfur to form pyrite.[8, 47] Arsenian pyrites, as the most important gold-bearing minerals, are formed by hydrothermal fluids, in which Fe are mainly contributed by ferroandolomite or other Fe-bearing minerals in the country rocks. The reduced S in the hydrothermal fluids coming from the magmatic source or sedimentary rocks are responsible for transporting Au during the sulfidation process, which is the most important process accompanied with the precipitation of gold and lead to the close relationship between hydrothermal pyrites and gold.

4.3. Elements Geochemistry

The REE analyses results of ore and wall rock were chondrite-normalized by using the data of Sun and McDonough[48] and shown in Table II and Figure 9.[48] Samples from the three deposits show appropriate incline REE patterns, demonstrating the enrichment of light rare element (LREE) and relatively flat heavy rare earth element (HREE).

The ΣREE of argillite and bioclastic limestone from Shuiyindong gold deposit ranges from 226 ppm to 465 ppm with an average of 306 ppm, along with LREE/HREE = 3.86–5.12 (average 4.55), La_N/Yb_N = 14.7–11.8 (average 13.4), respectively. For the Nibao gold deposit, the tuff samples have ΣREE = 239–293 ppm, with an average of 263 ppm, LREE/HREE = 3.42–4.62, with an average of 3.98 and La_N/Yb_N = 10.4–12.8, with an average of 11.4. Silicified limestone from SBT of Getang gold deposit ΣREE= 14.8–25.9 ppm, with an average of 19.6 ppm, LREE/HREE = 2.85–6.77, with an average of 4.46 and La_N/Yb_N = 13.7–34.9, with an average of 22.8.

The average value of La_N/Yb_N for Nibao deposit is the closest to that of the Emeishan basalts. The La_N/Yb_N

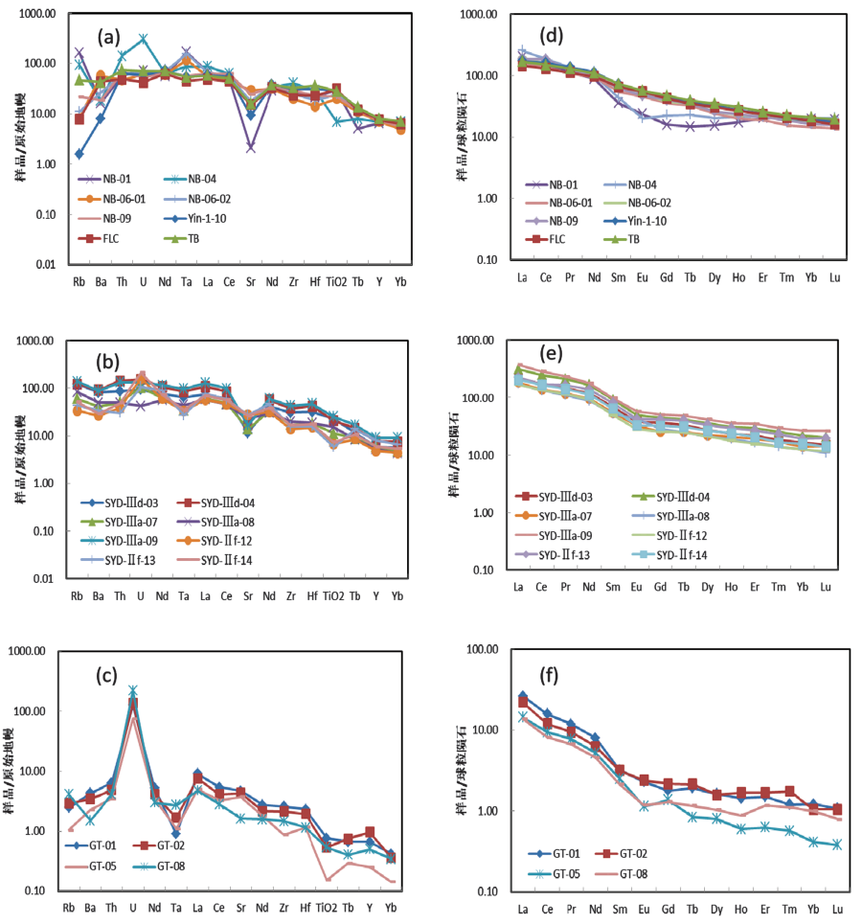

Figure 9. Primitive mantle-normalized spidergrams (a–c) and chondrite-normalized REE distribution patterns for samples (d–f) (normalized by the data of Sun and McDonough[48]).

ratios of the Getang (average 22.9) are apparently higher than those of the Shuiyingdong (average 13.4) and Nibao (average 11.4), indicating a different degree of fractionation of REEs during the hydrothermal alteration. All the δEu and δCe of the three deposits show obvious slight negative anomalies, except for the SYD-08, in which the δEu show a slight positive anomaly. The δEu and δCe average values of Emeishan basalts are 0.99 and 1.02 respectively, showing slight to no anomalies ($\delta Eu = Eu_N/[1/2(Sm_N + Gd_N)]$; $\delta Ce = Ce_N/[1/2(La_N + Pr_N)]$, N repents the chondrite-normalized data).

Similar to the Emeishan basalts, the clastic rocks and tuff samples from the Shuiyindong and Nibao deposits show right incline REE patterns, enrichment of LREE and flat HREE. In addition, the tuff samples from the Nibao deposit have a more similar geochemical behavior with the Emeishan basalts. They all show slightly enrichment of Nd and positive anomalies of Ta and δEu, suggesting that the Emeishan basalts may provide ore-forming material source partially. Moreover, the LREE/HREE of the Nibao deposit (average 3.98) is less than the Shuiyindong (average 4.55) and Getang deposits (average 4.46), indicating that there may be some deep source material participated in mineralization because the deep source material have a much lower LREE/HREE. According to data statistics of all samples, we mapped a ΣREE-La/Yb diagram and found that the samples from the Getang deposit are in the area of mudstone and the samples from the Shuiyindong and Nibao deposits are close to the overlap region of alkali basalt and mudstone (Fig. 10).[49] All these results indicate that deep substance may participate in the ore-forming process of Shuiyindong and Nibao deposits. Previous isotope studies on the Shuiyindong deposit also indicated that the

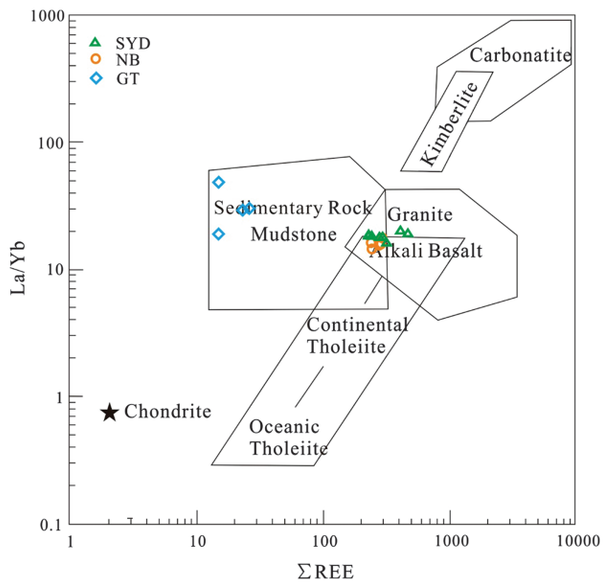

Figure 10. ΣREE—La/Yb (modified after Liao et al.[49]) of samples from Shuiyindong, Nibao and Getang gold deposits

ore-forming fluid for the main mineralization stage could have been derived mainly from a magmatic source and mixed with certain meteoric water. The $\delta^{34}S$ values of sulfide in various mineralization stages suggest that the sulfur of hydrothermal sulfides was likely mixtures of magmatic source with minor contribution of sedimentary rocks (e.g., dissolution of diagenetic pyrite).[39,47] While, the $\delta^{34}S$ of the gold-bearing pyrites in the Nibao deposit is average −0.40‰, indicating a characteristic of magmatic source.[30]

The REE of the samples from Getang deposit are lower than those from the Shuiyindong and Nibao deposits because more clay and tuffaceous exist in the Shuiyindong and Nibao deposits, which implies the difference in metallogenic mechanism and ore-forming material source of the three deposits. The isotopic compositions of hydrothermal minerals reported by Zhang et al.[27] showed that most of sulfur in the Getang deposit might derive from the sedimentary rocks and the hydrothermal fluids responsible for gold mineralization were deduced to be a deep circulated metamorphic fluid with additional meteoric water through deep fractures.[27]

5. CONCLUSION

Based on textural analyses and trace element distribution, pyrite can be divided into depositional pyrite and hydrothermal pyrite. Depositional pyrite was produced by synsedimentary or early diagenesis. As the major gold-bearing minerals in the three deposits, arsenian pyrites are formed during hydrothermal processes. The involvement of the hydrothermal pyrites is closely related to the enrichment of gold, in which the fluid should be enriched in Au and As, but depleted in Fe.

Three types of invisible gold were observed in the three Carlin-gold deposits i.e., nanoparticles, submicroscopic particles, and lattice gold. Au nanoparticles and submicroscopic particles mostly distribute in arsenian pyrite veinlet or quartz, while lattice gold always present as crystal lattice in the overgrowth rims of arsenian pyrite. In the Carlin-type gold deposits, the saturation of gold-bearing solution, decarbonatization and sulfidation are the most important factors that affect the transport and deposition mechanisms of gold. Au mostly migrates as Au^{+1} or Au^0, which is seriously affected by the saturation of gold-bearing solution. Decarbonatization and sulfidation are responsible to provide the Fe and S to form hydrothermal pyrite, which is the most important minerals coprecipitate with gold.

Mineralized rocks from the three deposits display LREE enrichment patterns. The consistency of geochemical behavior among Shuiyindong, Nibao deposits and typical Emeishan basalt indicates that the two deposits may be affected by basic volcanic clastic material during sedimentation. The element geochemistry of samples from Getang deposit is much different from the other two

deposits and sedimentary rocks maybe play a significant role in the ore-forming process.

Acknowledgment: The study was supported financially by the Major State Basic Research Development Program of China (973 Program) (2014CB440906). Comments from reviewers were very helpful and valuable. We are also grateful to the Guizhou Zijin gold mine for access to the mine.

References and Notes

1. G. B. Arehart, *Ore Geology Reviews* 11, 383 (**1996**).
2. A. H. Hofstra and J. S. Cline, *Economic Geology* 13, 163 (**2000**).
3. A. H. Hofstra, L. W. Snee, R. O. Rye, H. W. Folger, J. D. Phinisey, R. J. Loranger, A. R. Dahl, C. W. Naeser, H. J. Stein, and M. Lewchuk, *Economic Geology*. 94, 769 (**1999**).
4. J. S. Cline, A. H. Hofstra, J. L. Muntean, R. M. Tosdal, and K. A. Hickey, Economic Geology 100th Anniversary Volume 451 (**2005**).
5. R. Z. Hu, W. C. Su, X. W. Bi, G. Z. Tu, and A. H. Hofstra, *Mineralium Deposita* 37, 378 (**2002**).
6. G. Z. Tu, *Acta Geologica Sichuan* 12, 1 (**1992**).
7. Y. Xia, Y. Zhang, W. C. Su, Y. Tao, X. C. Zhang, J. Z. Liu, and Y. M. Deng, *Acta Geologica Science* 83, 1473 (**2009**).
8. W. C. Su, C. A. Heinrich, T. Pettke, X. C. Zhang, R. Z. Hu, and B. Xia, *Economic Geology* 104, 73 (**2009**).
9. F. Daliran, *Mineralium Deposita* 43, 383 (**2008**).
10. J. S. Cline, J. L. Muntean, and X. X. Gu, *Earth Science Frontiers* 20, 1 (**2013**).
11. P. Emsbo, A. H. Hofstra, E. A. Lauha, G. L. Griffin, and R. W. Hutchinson, *Economic Geology and the Bulletin of the Society of Economic Geologists* 98, 1069 (**2003**).
12. R. R. Large, L. Danyushevsky, C. Hollit, V. Maslennikov, S. Meffre, S. Gilbert, S. Bull, R. Scott, P. Emsbo, H. Thomas, B. Singh, and J. Foster, *Economic Geology* 104, 635 (**2009**).
13. R. R. Large, S. W. Bull, and V. V. Maslennikov, *Economic Geology* 106, 331 (**2011**).
14. M. H. Chen, J. W. Mao, C. Li, Z. Q. Zhang, and Y. Dang, *Ore Geology Reviews* 64, 316 (**2015**).
15. Y. J. Tan, *Geology of Carlin-Type Gold Deposits in the Dian-Qian-Gui Area*, Nanjing University Press, Nanjing (**1994**).
16. G. S. Huang and Y. Y. Du, *Geology of Guizhou* 10, 1 (**1993**).
17. Q. Y. Ran and Z. G. Yang, *Geology of Guizhou* 12, 208 (**1995**).
18. G. B. Arehart, S. L. Chryssoulis, and S. E. Kesler, *Economic Geology* 88, 171 (**1993**).
19. G. Simon, H. Huang, J. E. Penner-Hahn, S. E. Kesler, and L. S. Kao, *American Mineralogist* 84, 1071 (**1999**).
20. C. S. Palenik, S. Utsunomiya, M. Reich, S. E. Kesler, L. M. Wang, R. C. Ewing. *American Mineralogist* 89, 1359 (**2004**).
21. M. Reich, S. E. Kesler, S. Utsunomiya, C. S. Palenik, S. L. Chryssoulis, and R. C. Ewing, *Geochimica et Cosmochimica Acta* 69, 2781 (**2005**).
22. J. Z. Liu, Y. Xia, X. C. Zhang, Y. M. Deng, W. C. Su, and Y. Tao, *Gold Science and Technology* 16, 1 (**2008**).
23. Z. W. Bao, Z. H. Zhao, J. Guha, and A. E. Williams-Jones, *Geochemical Journal* 38, 363 (**2004**).
24. Z. J. Han, Y. G. Wang, J. Z. Feng, T. J. Chen, and Y. H. Liu, Geology and exploration of sedimentary-rock-hosted disseminated gold deposits in southern Guizhou, Guizhou Science and Technology Publishing House, Guiyang (**1999**).
25. Y. G. Wang, *Lithofacies Paleo-Geography* 6, 8 (**1990**).
26. S. G. Peters, J. Z. Huang, Z. P. Li, and C. G. Jing, *Ore Geology Reviews* 31, 170 (**2007**).
27. X. C. Zhang, B. Spiro, C. Halls, C. J. Stanley, and K. Y. Yang, *International Geology Review* 45, 407 (**2003**).
28. W. C. Su, H. T. Zhang, R. Z. Hu, X. Ge, B. Xia, Y. Y. Chen, and C. Zhu, *Mineralium Deposita* 47, 653 (**2012**).
29. Q. P. Tan, Y. Xia, Z. J. Xie, and J. Yan, *Ore Geology Reviews* 69, 140 (**2015**).
30. P. Liu, P. G. Li, R. Ma, Z. H. Han, G. L. Yang, and D. S. Ye, *Mineral Deposits* 25, 101 (**2006**).
31. L. L. Zheng, R. D. Yang, J. Z. Liu, J. B. Gao, J. Chen, and J. H. Li, *Geology and Eeploration* 50, 689 (**2014**).
32. J. Z. Liu, C. F. Yang, Y. Xia, S. Chen, F. E. Chen, You B, and Z. K. Fu, *Geology of Guizhou* 27, 178 (**2010**).
33. J. G. Huang, H. J. Li, W. J. Li, and L. Dong, *Geology of China* 39, 1318 (**2012**).
34. L. Qi and D. C. Gregoire, *Geostandards Newsletter-the Journal of Geostandards and Geoanalysis* 24, 51 (**2000**).
35. I. B. Butler and D. Rickard, *Geochimica et Cosmochimica Acta* 64, 2665 (**2000**).
36. G. S. Pokrovski, S. Kara, and J. Roux, *Geochimica et Cosmochimica Acta* 66, 2361 (**2002**).
37. M. Blanchard, M. Alfredsson, J. Brodholt, K. Wright, and C. R. A. Catlow, *Geochimica et Cosmochimica Acta* 71, 624 (**2007**).
38. C. H. Zhao, Sulfide Mineralogy and Genetic Model of the Lannigou Carlin-Type Gold Deposit in Southwestern Guizhou, China, Unpublished Ph.D. Thesis, Institute of Geochemistry, Chinese Academy of Sciences, Guizhou, China (**2014**).
39. L. Hou, H. J. Peng, J. Ding, J. R. Zhang, S. B. Zhu, S. Y. Wu, and H. G. Ouyang, *Economic Geology* 111, 331 (**2016**).
40. A. Bralia, G. Sabatini, and F. Troja, *Mineralium Deposita* 14, 353 (**1979**).
41. W. C. Su, B. Xia, H. T. Zhang, X. C. Zhang, and R. Z. Hu, *Ore Geology Reviews* 33, 667 (**2008**).
42. A. Usher, D. C. McPhail, and J. Brugger, *Geochimica et Cosmochimica Acta* 73, 3359 (**2009**).
43. M. E. Fleet, P. J. MacLean, and J. Barbier, *Economic Geology, Monograph* 6, 356 (**1989**).
44. A. Cepedal, M. Fuertes-Fuente, A. Martin-Izard, S. Gonzalez-Nistal, and M. Barrero, *Canadian Mineralogist* 46, 233 (**2008**).
45. L. M. Maddox, G. M. Bancroft, M. J. Scaini, and J. W. Lorimer, *American Mineralogist* 83, 1240 (**1998**).
46. M. J. Scaini, G. M. Bancroft, and S. W. Knipe, *American Mineralogist* 83, 316 (**1998**).
47. Q. P. Tan, Y. Xia, Z. J. Xie, J. Yan, and D. T. Wei, *Chinese Journal of Geochemistry* 34, 525 (**2015**).
48. S. S. Sun and W. F. McDonough, Chemical and Isotopic Systematics of Oceanic Basalts: Implications for Mantle Composition and Processes, Geological Society, London (**1989**).
49. Z. M. Liao, L. Y. Ma, and P. Tao, *Geology of Guizhou* 31, 10 (**2014**).

Received: 3 April 2016. Accepted: 3 September 2016.